

1 Lessons learned from oxygen isotopes in modern precipitation applied to interpretation of
2 speleothem records of paleoclimate from eastern Asia

3
4 Katherine E. Dayem^{a*}, Peter Molnar^b, David S. Battisti^c, Gerard H. Roe^d,

5
6 a. Department of Geological Sciences and Cooperative Institute for Research in
7 Environmental Sciences (CIRES), University of Colorado, Campus Box 399, Boulder,
8 Colorado 80309, USA. dayem@colorado.edu, phone: +1 (303) 492-7296, fax: +1 (303)
9 492-2606

10 b. Department of Geological Sciences and Cooperative Institute for Research in
11 Environmental Sciences (CIRES), University of Colorado, Campus Box 399, Boulder,
12 Colorado 80309, USA. molnar@colorado.edu

13 c. Department of Atmospheric Sciences, University of Washington, Box 351640, Seattle,
14 Washington 98195-1640, USA. battisti@u.washington.edu

15 d. Department of Earth and Space Sciences, University of Washington, Box 351310,
16 Seattle, Washington 98195, USA. gerard@ess.washington.edu

17
18 * corresponding author

19
20
21

22 Abstract

23 Variability in oxygen isotope ratios collected from speleothems in Chinese caves
24 is often interpreted as a proxy for variability of precipitation, summer precipitation,
25 seasonality of precipitation, and/or the proportion of ¹⁸O to ¹⁶O of annual total rainfall
26 that is related to a strengthening or weakening of the East Asian monsoon and, in some
27 cases, to the Indian monsoon. We use modern reanalysis and station data to test whether
28 precipitation and temperature variability over China can be related to changes in climate
29 in these distant locales. We find that annual and rainy season precipitation totals in each
30 of central China, south China, and east India have correlation length scales of ~500 km,
31 shorter than the distance between many speleothem records that share similar long-term
32 time variations in $\delta^{18}\text{O}$ values. Thus the short distances of correlation do not support,
33 though by themselves cannot refute, the idea that apparently synchronous variations in
34 $\delta^{18}\text{O}$ values at widely spaced (>500 km) caves in China are due to variations in annual

35 precipitation amounts. We also evaluate connections between climate variables and $\delta^{18}\text{O}$
36 values using available instrumental measurements of $\delta^{18}\text{O}$ values in precipitation. These
37 data, from stations in the Global Network of Isotopes in Precipitation (GNIP), show that
38 monthly $\delta^{18}\text{O}$ values generally do not correlate well with either local precipitation
39 amount or local temperature, and the degree to which monthly $\delta^{18}\text{O}$ values do correlate
40 with them varies from station to station. For the few locations that do show significant
41 correlations between $\delta^{18}\text{O}$ values and precipitation amount, we estimate the differences in
42 precipitation amount that would be required to account for peak-to-peak differences in
43 $\delta^{18}\text{O}$ values in the speleothems from Hulu and Dongge caves, assuming that $\delta^{18}\text{O}$ scales
44 with the monthly amount of precipitation or with seasonal differences in precipitation.
45 Insofar as the present-day relationship between $\delta^{18}\text{O}$ values and monthly precipitation
46 amounts can be applied to past conditions, differences of at least 50% in mean annual
47 precipitation would be required to explain the $\delta^{18}\text{O}$ variations on orbital time scales,
48 which are implausibly large and inconsistent with published GCM results. Similarly,
49 plausible amplitudes of seasonal cycles in amounts or in seasonal variations in $\delta^{18}\text{O}$
50 values can account for less than half of the 4-5‰ difference between glacial and
51 interglacial $\delta^{18}\text{O}$ values from speleothems in China. If seasonal cycles in precipitation
52 account for the amplitudes of $\delta^{18}\text{O}$ values on paleoclimate timescales, they might do so
53 by extending or contracting the durations of seasons (a frequency modulation of the
54 annual cycle), but not by simply varying the amplitudes of the monthly rainfall amounts
55 or monthly average $\delta^{18}\text{O}$ values (amplitude modulation). Allowing that several processes
56 can affect seasonal variability in isotopic content, we explore the possibility that one or
57 more of the following processes contribute to variations in $\delta^{18}\text{O}$ values in Chinese cave

58 speleothems: different source regions of the precipitation, which bring different values of
59 $\delta^{18}\text{O}$ in vapor; different pathways between the moisture source and the paleorecord site
60 along which exchange of ^{18}O between vapor, surface water, and condensate might differ;
61 a different mix of processes involving condensation and evaporation within the
62 atmosphere; or different types of precipitation. Each may account for part of the range of
63 $\delta^{18}\text{O}$ values revealed by speleothems, and each might contribute to seasonal differences
64 between past and present that do not scale with monthly or even seasonal precipitation
65 amounts.

66

67 Keywords: monsoon; paleoclimate; oxygen isotope ratios; Asia; precipitation

68 1. Introduction

69 Oxygen isotopes measured in cave speleothems from China show systematic
70 variations that are related to orbitally paced variations in insolation (e.g., Wang et al.,
71 2001; Yuan et al, 2004; Zhang et al, 2008). Variability of the ratio of ^{18}O to ^{16}O in calcite
72 (measured as $\delta^{18}\text{O}$ values) on orbital time scales at four caves in China is $\sim 5\text{‰}$ at Hulu
73 cave (32.5°N , 119.1°E) (Yuan et al., 2004), ~ 5 to 6‰ at Dongge cave (25.3°N , 108.1°E)
74 (Wang et al., 2001), $\sim 4\text{‰}$ at Xiaobailong cave (24.2°N , 103.3°E) (Cai et al., 2006), and
75 $\sim 3\text{‰}$ at Heshang cave, a shorter record covering only the past ~ 9500 years (Hu et al.,
76 2008) (Fig. 1). Such variability in $\delta^{18}\text{O}$ values almost surely reflects differences in some
77 aspect of precipitation in China over the same time scale. Logical arguments can be made
78 that the isotopic composition of precipitation should depend on some of the following:
79 the amount of local precipitation that occurs on timescales as short as individual
80 rainstorms to as long as years, on temperature (possibly on similar timescales), on the
81 source of water vapor and changes in its temperature, and on the path followed by the
82 vapor including precipitation and evaporation along it. Essential to the interpretation of
83 paleoclimate records is an understanding of which of the factors listed above are
84 responsible for the $\delta^{18}\text{O}$ signals recorded in stalagmites. Our goal here it to improve that
85 understanding.

86 Paleoclimate records collected from caves in the subtropics in Israel (e.g. Bar-
87 Matthews et al., 2000, 2003), Oman (e.g., Burns et al., 2000; Fleitmann et al., 2003,
88 2004), India (Sinha et al. 2005, 2007), South America (Cruz et al., 2009), and Borneo
89 (Partin et al., 2007) have been have been interpreted as proxies for local precipitation
90 amount, and some assume the same (“amount of summer monsoon precipitation”) for

91 China (e.g., Cai et al., 2010; Zhou et al., 2007). Others argue that isotopic variability
92 does not imply differences in precipitation amount; rather it indicates changes in the ratio
93 of summer to winter precipitation, which they refer to as ‘monsoon intensity’ (e.g., Cai et
94 al., 2006; Cheng et al., 2006, 2009; Dykoski et al., 2005; Kelly et al., 2006; Wang et al.,
95 2008; Yuan et al., 2004). Their logic is that $\delta^{18}\text{O}$ values in modern spring rainfall are less
96 negative than those in modern summer rainfall. In the annual mean, more summer
97 rainfall should lead to more negative annual weighted $\delta^{18}\text{O}$ values. Thus in interpreting a
98 $\delta^{18}\text{O}$ record as a proxy for summer monsoon intensity, these authors implicitly assume
99 that the same seasonal moisture sources and transport pathways have prevailed in the
100 past, but their relative contributions to the annual average $\delta^{18}\text{O}$ values have varied.

101 Johnson and Ingram (2004) examine the relationship between $\delta^{18}\text{O}$ values
102 measured in precipitation and the *in situ* temperature and precipitation. They regress $\delta^{18}\text{O}$
103 values against the annual cycle in local temperature and precipitation using data from
104 three continuous years at 10 stations over China. They conclude that, to the extent the
105 processes controlling $\delta^{18}\text{O}$ values in the modern climate are relevant to those in past
106 climates, the $\delta^{18}\text{O}$ variations in the caves should be interpreted as a proxy record of a
107 combination of temperature and precipitation. More recently, extending these results,
108 Johnson et al. (2006b) argue that changes in monsoon intensity could contribute
109 significantly to the orbital scale variations in the speleothem $\delta^{18}\text{O}$ values, but they go on
110 to conclude that, most likely, the dominant process contributing to the orbital scale
111 variations in the $\delta^{18}\text{O}$ in the cave records is changes in the pathway and processing of
112 moisture from the evaporation source to the cave sites.

113 Currently, there is a widespread belief that the oxygen isotopes measure some
114 aspect of the strength or intensity of the monsoon, but apparent differences in usage of
115 words such as strength and intensity has complicated interpretations of such isotopic data
116 in terms of variations in climate. As noted above, many equate monsoon intensity to the
117 ratio of summer to winter rainfall amount that is local to the cave site, but the use of
118 adjectives like “strong” or “weak” to describe paleo-monsoons, coupled with the explicit
119 association of large negative $\delta^{18}\text{O}$ values with local summertime precipitation has led to
120 some confusion within the paleoclimate community of how $\delta^{18}\text{O}$ values relate to past
121 climate and what atmospheric feature(s) is implied when the term “monsoon” is used. In
122 a recent example, Cheng et al. (2009, p. 249) define explicitly what they mean by
123 “monsoon intensity,” but in commenting on the paper, Severinghaus (2009) seems to
124 ignore that definition and summarizes the work of Cheng et al. as “a record of past
125 monsoon strength.” We prefer to frame our analysis in terms of rainy and dry seasons,
126 and in the discussion below comparing our modern climate analysis with paleoclimate
127 record interpretation, we will use the term monsoon to refer to the seasonal *circulation* in
128 China.

129 In eastern China, high-resolution records of oxygen isotopes from cave
130 speleothems provide climate data back to 224 kyr (e.g., Wang et al., 2008). Speleothems
131 from cave stalagmites record $\delta^{18}\text{O}$ values that are determined by the $\delta^{18}\text{O}$ value of the
132 precipitation and by any fractionation that may occur in the aquifer and during calcite
133 precipitation in the cave (Fairchild et al., 2006; Hendy, 1971; Johnson et al., 2006a; Vaks
134 et al., 2003). We focus only on atmospheric process here, but call attention to detailed
135 studies of the isotopic composition of modern dripwater in Chinese caves to assess the

136 degree to which fractionation and mixing may occur on the oxygen's path from
137 precipitation to speleothem, such as that of Johnson et al. (2006a).

138 In this study we present further analysis of the modern climate and isotopic
139 precipitation data that supports the hypothesis that the orbital scale variability (as well as
140 the stadial-interstadial differences) in cave $\delta^{18}\text{O}$ values in China is most likely due to a
141 combination of processes that include differences in the $\delta^{18}\text{O}$ values in the source waters
142 and in the pathways and processing of moisture transport en route to the cave site and to
143 local differences in convective processes (and hence fractionation) but not in
144 precipitation amount. We focus on two questions. (1) What is the spatial extent of
145 covariability of temperature or precipitation? This pertains to the question: What is the
146 spatial scale of a climate anomaly that would be captured by the proxy stalagmite $\delta^{18}\text{O}$
147 values? (2) Can we better quantify the influence of local temperature and precipitation
148 amount on $\delta^{18}\text{O}$ values in precipitation in the modern climate? This provides a step
149 toward answering: what could $\delta^{18}\text{O}$ values at a site represent in climates of the past? To
150 answer (1), we examine the spatial extent of correlations of precipitation and temperature
151 of cave locations with the rest of Asia.

152 Following Johnson and Ingram (2004), we answer question (2) by correlating
153 $\delta^{18}\text{O}$ values with local precipitation and temperature. We then estimate precipitation in
154 the past assuming that the main influence on $\delta^{18}\text{O}$ values on paleoclimate time scales
155 arises from variations in precipitation amount, which we infer using correlations with
156 modern monthly $\delta^{18}\text{O}$ values, but without necessarily ascribing such correlations to the
157 "amount effect." Our analysis differs from Johnson and Ingram (2004) in that we use
158 longer data sets, calculate correlations using both monthly, annual cycle, and annually

159 averaged data, and we use more stations in the region impacted by the Meiyu front: the
160 region commonly associated with the East Asian monsoon. If significant relationships
161 between $\delta^{18}\text{O}$ values and precipitation or temperature do not exist in present-day data,
162 relationships between those variables in the lower frequency paleorecords may still exist,
163 but, if so, they suggest that the fundamental processes that are responsible for variability
164 in the present-day climate are different from those in the distant past. Conversely,
165 modern variability offers tests of the hypothesized explanations for variability in the cave
166 $\delta^{18}\text{O}$ signals that, if they pass, can give support for such explanations.

167 Our approach is undoubtedly simplistic. Modern isotope ratios may depend not
168 only on temperature, precipitation rate, and horizontal and vertical distance from the
169 moisture source, but also on the moisture recycling on the continents (e.g., Gat, 1996),
170 precipitation rate and raindrop size (e.g., Lee and Fung, 2008), and atmospheric
171 circulation – the agent that transports moisture from source to precipitation site (e.g.,
172 Cobb et al., 2007; Dansgaard, 1964; Johnson et al., 2006b; Kelly et al., 2006; Lee et al.,
173 2007; Rozanski et al., 1992; Wang et al., 2001). In essence, to understand the variability
174 of an oxygen isotope ratio signal we need to know how atmospheric processes affect
175 isotopic ratios in precipitation, and which of these processes have the largest influence on
176 the isotope signal. Precipitation and temperature observations are easy to obtain and
177 hence our first test is for covariability of these variables with $\delta^{18}\text{O}$ values. The lack of a
178 significant relationship would indicate that the dominant control on $\delta^{18}\text{O}$ values is
179 another process, or that no single dominant process, or simple set of processes, exists.
180

181 2. Spatial extent of modern climate variability

182 Tropical and mid-latitude regions of Asia, such as northern India and southeast
183 China, receive large amounts of precipitation, even in the annual mean (Fig. 2). We test
184 whether variations in annual precipitation are coherent across broad regions in China and
185 India by correlating annual mean precipitation and temperature at sites near Hulu,
186 Dongge, and Dandak (East India) caves, where $\delta^{18}\text{O}$ records have been collected from
187 cave speleothems (e.g., Sinha et al., 2007; Wang et al., 2001; Yuan et al., 2004), with
188 precipitation and temperature at all other points in Asia. Temperature and precipitation
189 are from the NCAR/NCEP reanalysis data set (e.g., Kalnay et al., 1996). We carried out
190 the same analysis using data from the ECMWF ERA-40 data set (Uppala et al., 2005) and
191 obtained similar results to those we describe below.

192 The annually averaged (January to December) precipitation, which eliminates the
193 seasonal march in precipitation from south to north in eastern China, correlates positively
194 and significantly over only relatively small spatial scales (Fig. 3, left column). The
195 spatial scale of significant correlation is ~ 500 km near Hulu cave and slightly larger near
196 Dongge cave (Fig. 3c). Thus, in modern climate, a wet year near one cave does not
197 imply the same at the other cave. Precipitation on the east coast of India correlates with
198 precipitation over the whole of northern India, but hardly at all with anywhere in China
199 (Fig. 3e). The lack of significant correlation between precipitation near Hulu cave with
200 that near Dongge cave or East India, as well as none between the latter two sites, suggests
201 that processes that bring moisture to the Indian and southeast Asian monsoon regions are
202 broadly separate (e.g., Fasullo and Webster, 2003; Wang and Fan, 1999; Webster et al.,

203 1998), and that the processes that affect variability of precipitation in eastern China seem
204 to behave differently in its northern and southern parts (e.g., Lee et al., 2008).

205 The annually averaged temperature covaries over a larger region than does
206 precipitation (Fig. 3, right column). The temperature near Hulu cave correlates positively
207 and significantly with temperature along eastern China and north of the Tibetan plateau
208 (Fig. 3b). Temperature near Dongge cave covaries with temperature in southern China,
209 northern India, and north of the Tibetan plateau (Fig. 3d). Temperature in eastern India
210 correlates positively with that across India and southeastern Asia (Fig. 3f). Correlations
211 made using rainy season averaged temperature show similar patterns. Thus based only on
212 the modern record, one might expect that a local temperature record reflects variability
213 over a larger region than does a local precipitation record.

214 Our analysis suggests that precipitation anomalies are not correlated over an area
215 large enough to account for the high correlation in the cave $\delta^{18}\text{O}$ records on orbital time
216 scales to precipitation through a local amount effect. Hence, for the coherence in the
217 $\delta^{18}\text{O}$ values in cave records to reflect changes in local precipitation on orbital time scales,
218 the response of the climate system to orbitally induced variation in insolation must be
219 different from the processes responsible for the natural variability in seasonal and annual
220 precipitation in the modern climate.

221

222 3. Seasonality of modern precipitation and temperature in eastern China

223 The seasonality of present-day precipitation in eastern China varies from south to
224 north (Fig. 1). Precipitation rates are maximum in late spring and early summer in
225 southeast China (stations Guilin, Hong Kong, Liuzhou, and to a lesser degree Fuzhou in

226 Fig. 1), but are maximum in mid- to late summer farther north (Nanjing and
227 Shijiazhuang, Fig. 1). This south to north progression of high precipitation rates follows
228 the path of the Meiyu front, a warm, humid, and convective subtropical frontal system
229 that is related to the subtropical high pressure system over the western Pacific Ocean
230 (Zhou et al., 2004 and references therein). The front stretches northeast to southwest
231 over southeast China, extends as far west as $\sim 105^{\circ}\text{E}$ and as far north $\sim 35^{\circ}\text{N}$ (Zhou et
232 al., 2004) (Fig. 1). Only two of the stations we examine lie outside the Meiyu front
233 region: Shijiazhuang is north of the northernmost edge of the front, and Kunming is west
234 of the region affected by frontal dynamics (Fig. 1). Stations at Guiyang and Zunyi, on
235 the western edge of the Meiyu front region, receive maximum precipitation rates in the
236 early summer rather than in the spring (Fig. 1). Low-level winds associated with Meiyu
237 frontal precipitation are generally from the south. Coastal stations Hong Kong and
238 Fuzhou receive high precipitation rates both as the Meiyu front impacts them in late
239 spring to early summer and again in late summer after the Meiyu front has moved
240 northward. These later high precipitation rates are associated with easterly winds (not
241 shown) and may result, at least in part, from local differential land-sea heating. We
242 stress, however, that the majority of the precipitation in southeast China is associated
243 with frontal dynamics, convection, and convergence of the large-scale circulation.

244

245 4. Correlation of $\delta^{18}\text{O}$ values with precipitation and temperature

246 We wish to test the hypothesis that $\delta^{18}\text{O}$ values in precipitation scale either with
247 the amount of *in situ* precipitation or with *in situ* temperature. To do so, we use data
248 from GNIP stations (IAEA/WMO, 2004) in eastern China (Fig. 1) to calculate

249 correlations of monthly and of 12-month and 24-month running average values of $\delta^{18}\text{O}$ in
250 precipitation with local temperature and precipitation. Although modern $\delta^{18}\text{O}$ data is
251 limited to as few as 5 years at some stations with a maximum of 35 years at Hong Kong,
252 we expect that if robust relationships between $\delta^{18}\text{O}$ values and precipitation or
253 temperature exist, even these short term modern records should show systematic
254 correlations with climate variables. Correlations on the monthly time scale contain
255 information on present-day atmospheric variability. Correlations using one- or two-year
256 running average data may better reflect the atmospheric variability recorded in cave
257 speleothems, as the latter reflect a smoothed version of $\delta^{18}\text{O}$ values in precipitation due to
258 the retention time in the soil above a cave (e.g., Johnson et al., 2006a; Vaks et al., 2003).
259 We also report correlations between anomalies (differences between monthly values and
260 the corresponding average monthly value) of the same variables, to remove correlations
261 associated with the seasonal cycle. In the remainder of this section, we show that where
262 significant correlations exist, monthly correlations between $\delta^{18}\text{O}$ values and temperature
263 or precipitation vary from station to station and explain less than 50% of the variance in
264 all cases. In general, temperature is better (anti-) correlated with $\delta^{18}\text{O}$ values than is
265 precipitation. Correlations between 12- and 24-month running averages of the variables,
266 however, are generally not significant.

267 We recognize that the time scales that can be sampled with modern data are short
268 compared with the integrated time sampled by a single measurement of $\delta^{18}\text{O}$ in calcite
269 from a speleothem. Nevertheless, we are motivated by two views: first, amplitudes of
270 proxies of climate variability in the paleorecord commonly are comparable to, if not
271 smaller than, amplitudes of variability in modern monthly data; and second, the physical

272 processes that fractionate ^{18}O during evaporation and condensation and the mechanisms
273 by which the atmosphere transports it (the laws of physics) did not differ in the past, even
274 if boundary conditions were different. An understanding of the modern record, therefore,
275 is a prerequisite for interpreting the paleorecord, even where that understanding is
276 quantitatively limited.

277

278 4.1 Monthly correlations

279 On a seasonal cycle, temperature and $\delta^{18}\text{O}$ values covary (anti-phased) at most
280 sites. Temperature is maximum in summer and $\delta^{18}\text{O}$ values are smallest in the late
281 summer to early fall (Fig. 1). Values of $\delta^{18}\text{O}$ generally then become less negative in the
282 wintertime. Precipitation covaries with $\delta^{18}\text{O}$ values throughout southern China less well
283 than does temperature, for maximum precipitation occurs in late spring to early summer,
284 and $\delta^{18}\text{O}$ values reach a minimum in late summer (Fig. 1).

285 For the few stations that show a statistically significant relationship, monthly $\delta^{18}\text{O}$
286 values and precipitation amount are negatively correlated (Table 1). Plots of $\delta^{18}\text{O}$ values
287 versus monthly precipitation (Fig. 4) indeed show large scatter at most sites. Correlations
288 statistically significant from zero are found only at Guiyang, Hong Kong, Kunming, and
289 Zunyi. Correlation coefficients between monthly anomalies of $\delta^{18}\text{O}$ values and monthly
290 anomalies in precipitation are also negative, but are significantly different from zero only
291 at Hong Kong.

292 Figure 4 shows scatter plots of the monthly averaged values of $\delta^{18}\text{O}$ versus
293 temperature for all stations. Where correlations are significant (see Table 1), temperature
294 is negatively correlated with $\delta^{18}\text{O}$ values, except at Shijiazhuang, which lies north of the

295 Meiyu front region and is unaffected by Meiyu precipitation (Fig. 1). In contrast,
296 monthly anomalies of $\delta^{18}\text{O}$ values and temperature are positively correlated where the
297 correlation is significant, at Kunming and Shijiazhuang, the two stations unaffected by
298 the Meiyu front. These differences between correlations of raw monthly data and those
299 with the seasonal cycle removed suggest that the seasonal cycle contains much of the
300 information in the $\delta^{18}\text{O}$ signal. Thus we suspect that the correlations between $\delta^{18}\text{O}$
301 values and temperature result from correlations of each variable with some other
302 seasonally varying factor such as insolation, the large-scale atmospheric circulation, or
303 precipitation type (e.g., convective storms versus drizzle). If this is the case, it need not
304 be local temperature that determines $\delta^{18}\text{O}$ values, but instead some other independent
305 process that affects both temperature and the value of the $\delta^{18}\text{O}$ in the precipitation. Local
306 temperature is thus an indicator of – but not necessarily the cause of – changes in
307 processes elsewhere, and the latter determine the $\delta^{18}\text{O}$ that is being precipitated over
308 China. We also note that just as $\delta^{18}\text{O}$ values in the paleorecords decrease with increasing
309 summer insolation (Cai et al., 2006; Wang et al., 2001; Yuan et al., 2004) and hence
310 presumably with increasing local temperature, modern $\delta^{18}\text{O}$ values decrease with
311 increasing temperature. This tendency, however, is opposite that expected from the
312 temperature dependence in Rayleigh fractionation: ^{18}O passes more readily from vapor to
313 condensate when the air is saturated and the temperature decreases (e.g., Dansgaard,
314 1964). The lack of agreement between trends in modern $\delta^{18}\text{O}$ values and expectations
315 based on Rayleigh fractionation has been observed globally in both observations and
316 model results (e.g., Brown et al., 2008; Lee et al., 2007), though a part of this poor

317 agreement stems from re-evaporation of liquid water. In any case, other processes must
318 conspire with Rayleigh fractionation to yield the recorded $\delta^{18}\text{O}$ values.

319 All sites in our study receive most of their precipitation in spring and/or summer,
320 which means that monthly average temperature and precipitation are positively
321 correlated. To test whether the lack of independence between precipitation and
322 temperature affects the correlations above, we calculate partial correlation coefficients for
323 the monthly mean time series, which remove the influence of either temperature or
324 precipitation (e.g., Arkin and Colton, 1970). For example, the partial correlation
325 $\rho(\delta^{18}\text{O}, T, P)$ is the correlation between $\delta^{18}\text{O}$ values and temperature with the effect of the
326 correlation between temperature and precipitation removed. Where significant, partial
327 correlation coefficients have the same sign and tend to be slightly smaller in magnitude
328 than the correlation coefficients (Table 1), suggesting that correlations between
329 temperature and precipitation affect correlations between $\delta^{18}\text{O}$ values and temperature or
330 precipitation by only small amounts.

331

332 4.2 Interannual correlations

333 For comparison to paleoclimate records, correlations between longer time
334 intervals may be more appropriate than monthly values. Therefore we calculate
335 correlations between the 12-month and 24-month running average values of $\delta^{18}\text{O}$ and the
336 corresponding averages of precipitation and temperature. Note that in calculating 12- and
337 24-month averages of $\delta^{18}\text{O}$ values, we use the monthly values of $\delta^{18}\text{O}$ weighted by the
338 amount of the precipitation that fell during that month and denoted by $\delta^{18}\text{O}_w$. To assess
339 statistical significance, we use an effective degrees of freedom $n - 2$ where n is the

340 number of years of data for 12-month averages and half that number for 24-month
341 averages. No correlations are significant at the 95% confidence level. Only the
342 correlations between 12- and 24-month running average values of $\delta^{18}\text{O}_w$ and temperature
343 at Hong Kong are significant at the 80% confidence level ($r = -0.30$ for 12-month
344 averages, and $r = -0.45$ for 24-month averages), which is suggestive at best. Thus, the
345 available instrumental record neither supports nor excludes the possibility of a
346 relationship between local climate variables and $\delta^{18}\text{O}_w$ values in precipitation.

347 A recent record of $\delta^{18}\text{O}$ values from a cave speleothem does, however, show that
348 $\delta^{18}\text{O}$ values covary with local temperature and precipitation amount for the past 50 years.
349 Zhang et al. (2008) calculated correlation coefficients of $\delta^{18}\text{O}$ values measured in
350 Wangxiang cave from 1950 to 2000 with 5-year running average precipitation ($r = -0.64$)
351 and temperature ($r = 0.8$) from a weather station ~15 km from the cave (Zhang et al.,
352 2008, Fig. S4). The magnitude of the interannual variations of the Wangxiang $\delta^{18}\text{O}$
353 values (~0.3‰) is small compared to monthly variations of GNIP data (~6-10‰) and
354 orbital variations of paleoclimate data (~5‰). Note also that the correlation between
355 $\delta^{18}\text{O}$ values and precipitation is of the same sign sense as the modern data, but that
356 between $\delta^{18}\text{O}$ values and temperature is the opposite. If a paleoclimate record responds
357 similarly to the recent part of the Wangxiang record, then it may be a good indicator of
358 local precipitation. Because the magnitude of variation in the Wangxiang record is so
359 much smaller than orbitally related variations, however, processes other than local
360 precipitation amount must account for the orbitally induced variations in cave $\delta^{18}\text{O}$
361 values at this site. Beyond waiting for longer timeseries of isotope measurements to
362 become available, another approach to build confidence in the correct climatic

363 interpretation of the speleothem record may be to exploit climate model studies that test
364 how $\delta^{18}\text{O}$ values in precipitation respond to various atmospheric processes (e.g., Bony et
365 al., 2008; Lee et al., 2007; Lee and Fung, 2008; Risi et al., 2008).

366

367 5. Discussion

368 Monthly correlations suggest that variations in $\delta^{18}\text{O}$ values generally correlate
369 better with temperature than with precipitation. At all stations except Shijiazhuang, $\delta^{18}\text{O}$
370 values are negatively correlated with temperature: rainwater is isotopically lighter when
371 temperature is higher (in summer). This negative relationship is like that of orbitally
372 induced changes in paleoclimate records, in that $\delta^{18}\text{O}$ values are more depleted during the
373 warmer periods (e.g., Cai et al., 2006; Wang et al., 2001; Yuan et al., 2004), but opposite
374 to that predicted by the temperature dependence in Rayleigh fractionation and to that
375 observed by Zhang et al. (2008) in a modern speleothem record, which they attribute to
376 global climate change. For northern and western stations (Guiyang, Kunming, Nanjing,
377 Shijiazhuang, and Zunyi), maximum temperature and lighter (most negative) $\delta^{18}\text{O}$ values
378 also correspond to the maximum precipitation rate (Fig. 1). Locations in southeast China
379 such as Guilin and Liuzhou receive maximum precipitation in spring or early summer but
380 minimum $\delta^{18}\text{O}$ values and maximum temperatures occur in late summer, so that $\delta^{18}\text{O}$ is
381 more negatively correlated to temperature than to precipitation. The correlations between
382 monthly anomalies of $\delta^{18}\text{O}$ values and precipitation or temperature, however, are small
383 and, with a few exceptions, insignificant. Thus, we infer that much of the variation in
384 $\delta^{18}\text{O}$ values results from seasonal variation of some process that may not depend directly
385 on local temperature or precipitation.

386 Partial correlation coefficients (Table 1) show that precipitation contributes to the
387 $\delta^{18}\text{O}$ signal in Hong Kong (which is influenced by a summer monsoon-like seasonal
388 precipitation), and to some extent at Shijiazhuang, which is north of the monsoon region
389 (Fig. 1; Table 1), in agreement with the analysis of Johnson and Ingram (2004). At these
390 and other sites, however, the partial correlation coefficients relating monthly values of
391 $\delta^{18}\text{O}$ to temperature are larger in magnitude than those for precipitation (Table 1).

392

393 5.1 Simple scaling analysis

394 A relationship between precipitation amounts or seasonal differences of
395 precipitation and $\delta^{18}\text{O}$ values can be tested using a simple scaling analysis that uses
396 estimates based on linear regressions of monthly $\delta^{18}\text{O}$ values versus monthly
397 precipitation amounts for stations with statistically significant correlations between them
398 (see Appendix A). In agreement with Johnson et al. (2006b) and Kelly et al. (2006), we
399 find that the difference between modern and last glacial maximum $\delta^{18}\text{O}$ values cannot be
400 explained by reasonable differences in the annual amount of local precipitation. For
401 example, to account for only a $\sim 1\text{‰}$ increase in $\delta^{18}\text{O}$ values, the difference between
402 modern and 9 ka $\delta^{18}\text{O}$ values at Dongge and Hulu caves (e.g., Wang et al., 2001; Yuan et
403 al., 2004), we find that the annually averaged precipitation at 9 ka would be at least 1.5
404 times greater than today (Appendix A).

405 Moreover, different seasonal amplitudes of precipitation amounts and of $\delta^{18}\text{O}$
406 values can account for part, but by no means all, of the 4-5‰ differences in $\delta^{18}\text{O}$ values
407 in caves, or the 3‰ difference between present-day and Last Glacial Maximum values at
408 Dongge cave (Dykoski et al., 2005). We address analysis of amplitude scaling in detail

409 in Appendix A, but consider the following simple calculation. Suppose, first, that today
410 $\delta^{18}\text{O}$ values averaged -6‰ during the 9 autumn, winter, and spring months and -10‰
411 during one 3-month season; second, suppose that roughly the same precipitation fell in
412 the three summer months as during the other nine months, so that the mean annual $\delta^{18}\text{O}$
413 value were $\sim -8\text{‰}$. (These values approximate those for Nanjing in Figure 1.) Now
414 suppose that in the past either the 3 summer months' precipitation did not occur at all or
415 it carried the same $\delta^{18}\text{O}$ values as the average for the other seasons; the resulting annual
416 average $\delta^{18}\text{O}$ value would have been -6‰ , only 2‰ different from that today. This,
417 obviously, is an extreme consideration, given the complete elimination of all of the most
418 negative $\delta^{18}\text{O}$ values, and that precipitation rates during some months when $\delta^{18}\text{O}$ values
419 are most negative are relatively low. Following the reasoning above and the more
420 rigorous calculations in Appendix A, we conclude that no plausible difference in the
421 amplitude of seasonal cycle of precipitation amount or its monthly $\delta^{18}\text{O}$ values can
422 account for even as much as half of variability of $\delta^{18}\text{O}$ values in the speleothems of
423 China.

424 GCM calculations of past climates also yield smaller glacial-interglacial
425 differences in $\delta^{18}\text{O}$ values than those reported in cave records (e.g., Hoffmann and
426 Heiman, 1997, Hoffmann et al., 2000, Jouzel et al., 1994) (Appendix B). Hence, neither
427 the GCM results nor the standard views of how $\delta^{18}\text{O}$ values vary in modern precipitation
428 can account for the full range of glacial-interglacial differences in $\delta^{18}\text{O}$ values, though
429 each can account for a part of that range.

430

431 5.2 Additional processes that may affect $\delta^{18}\text{O}$ values

432 The work of Johnson and Ingram (2004), Kelly et al. (2006), and Yuan et al.
433 (2004), along with the analysis above, point to changes in atmospheric circulation and in
434 moisture sources to explain the majority of the glacial-interglacial variation of $\delta^{18}\text{O}$
435 values of 4-5‰. Below we consider how glacial and interglacial $\delta^{18}\text{O}$ values might differ
436 at a cave site by assuming $\delta^{18}\text{O}$ values differences due to changes at the moisture source,
437 in the atmospheric circulation, and the storm type. The value of this exercise is not in the
438 specific $\delta^{18}\text{O}$ values we list (which are only rough estimates), but rather in the approach:
439 we hypothesize how atmospheric processes during past climates might have been
440 different from those of today, and estimate the potential for those processes to contribute
441 to the orbital scale variations in the cave records across China.

442

443 5.2.1. Moisture source

444 Ocean $\delta^{18}\text{O}$ values are enriched during glacial times, as lighter oxygen isotopes
445 are preferentially sequestered in glaciers and ice sheets. Mean glacial ocean $\delta^{18}\text{O}$ values
446 increase $\sim 1\text{‰}$ compared to interglacial ocean $\delta^{18}\text{O}$ values (e.g., Guilderson et al., 2001;
447 Schrag et al., 2002). Sea surface temperature is reduced by $\sim 2\text{-}3^\circ\text{C}$ in the South China
448 Sea during glacial periods (Oppo and Sun, 2005), however, and this may have led to a
449 $\sim 0.5\text{‰}$ decrease of $\delta^{18}\text{O}$ values in vapor sourced from that area. Thus the enrichment of
450 ^{18}O in vapor from the net of the ocean changes in glacial times is a relatively small \sim
451 0.5‰ .

452

453 5.2.2. Shifts in atmospheric circulation

454 Because of decreased insolation during glacial times, when colder conditions
455 prevailed especially at higher latitudes, the Meiyu front and the dynamics associated with
456 it might not have migrated as far north as it does today. To estimate the effect of this
457 southward contraction of the region affected by that front, we substitute summer $\delta^{18}\text{O}$
458 values for one station (Nanjing, for example) with those from a station farther north
459 (Shijiazhuang, for example), and we calculate that mean annual $\delta^{18}\text{O}$ values would
460 increase $\sim 1\text{‰}$ during glacial times. We offer this as one possible shift in atmospheric
461 circulation, but as discussed below, others seem just as plausible.

462

463 5.2.3. Rainstorm type

464 Precipitation from convective storms has been measured to have lower $\delta^{18}\text{O}$
465 values than non-convective precipitation (e.g., Lawrence and Gedzelman, 1996;
466 Lawrence et al., 2004; Risi et al., 2008; Scholl et al., 2009). For example, convective
467 rainfall during the monsoon in Niger is ~ -2 to -6‰ , whereas non-convective
468 precipitation before the monsoon is $\sim 0\text{‰}$ (Risi et al., 2008). Similarly, low $\delta^{18}\text{O}$ values
469 are also observed in China during the wet season (Fig. 1), when the area receives
470 convective precipitation related to the Meiyu front. Notice that except for Shijiazhuang
471 most of the months with the most negative $\delta^{18}\text{O}$ values are those with the largest mean
472 monthly temperatures (Fig. 4). If during glacial times, surface temperatures were 5°C
473 cooler than today, as studies elsewhere in the subtropics suggest (Stute et al., 1992,
474 1995), summer precipitation might have been denied the very low $\delta^{18}\text{O}$ values. Holmgren
475 et al. (2003) suggested the fraction of precipitation from convection may vary on

476 millennial time scales and this might account for isotopic differences in speleothems in
477 South Africa. Similarly, we hypothesize that convective rainfall, which scales with
478 radiative cooling of the atmosphere (e.g., Emanuel, 2007), is reduced during glacial
479 times. Using the monthly average values, we calculate annual weighted mean $\delta^{18}\text{O}$
480 values in which we eliminate months when precipitation is likely convective, and replace
481 those months with $\delta^{18}\text{O}$ values of months when precipitation is likely not convective. We
482 estimate annual weighted mean $\delta^{18}\text{O}$ values without convective rainfall could be $\sim 2\text{‰}$
483 heavier than modern mean annual $\delta^{18}\text{O}$ values.

484

485 It appears that none of the processes suggested above can, alone, account for the
486 4-5‰ difference between glacial and interglacial $\delta^{18}\text{O}$ values, and even their sum of \sim
487 3.5‰ seems to be too small. Part of this difference could be made up by seasonal
488 differences in precipitation amounts that do not depend on precipitation type, such as
489 what others have called ‘monsoon intensity’ (e.g., Cai et al., 2006; Cheng et al., 2006,
490 2009; Dykoski et al., 2005; Kelly et al., 2006; Wang et al., 2008; Yuan et al., 2004). In
491 any case, each of the estimates made above is approximate, and we offer them as
492 examples of how differences between modern and paleoclimate might account for
493 observed differences in $\delta^{18}\text{O}$ values. With better understanding of how modern $\delta^{18}\text{O}$
494 values are influenced by atmospheric circulation and mixing processes, hypothesized
495 circulation changes may be rejected or supported.

496

497 5.3. Durations of seasons

498 The analysis above and in Appendix A has assessed how varying the amplitude of
499 the seasonal cycle of precipitation could affect mean annual $\delta^{18}\text{O}$ values, which can be
500 seen as an amplitude modulation of the seasonal cycle. The high spectral power in the
501 precession band, however, raises the question of whether a better characterization of the
502 orbital forcing would exploit frequency modulation. As Huybers (2006) has shown,
503 Kepler's second law requires that the variation in durations of seasons play a key role in
504 how the earth's climate responds to orbital forcing.

505 So, suppose that instead of the amplitudes of seasonal precipitation amounts
506 and/or $\delta^{18}\text{O}$ values varied according to some seasonal cycle with a 1-year period,
507 durations of seasons changed, and with them so did $\delta^{18}\text{O}$ values (e.g., Cheng et al., 2009).
508 As an example, consider the case for Nanjing illustrated in Figure 1. Suppose that in
509 early Holocene time, when climate was warmest, the winter jet moved north across Tibet
510 not in May, as it does today (Schiemann et al., 2009), but in March. As an extreme
511 example, if summer rains like those currently in June, July, and August and $\delta^{18}\text{O}$ values
512 of -9‰ to -10‰, replaced those in April and May (with present-day values of -3‰ to -
513 4‰), the mean annual $\delta^{18}\text{O}$ values would differ by ~1‰, consistent with the difference
514 between early Holocene and present-day $\delta^{18}\text{O}$ values in caves. Similarly, if during glacial
515 times, the mid-latitude jet remained south of Tibet throughout much of the summer, and
516 if present-day springtime $\delta^{18}\text{O}$ values characterized those of summer months, the
517 calculated difference in mean annual $\delta^{18}\text{O}$ values between Last Glacial Maximum
518 conditions and the present-day would be more than 3‰. This too is an extreme
519 assumption for the seasonal differences in $\delta^{18}\text{O}$ values, but unpublished idealized General

520 Circulation Model calculations of K. Takahashi and Battisti (discussed briefly by Molnar
521 et al. (2010)) suggest that winter and spring rain result from the mid-latitude jet passing
522 south of Tibet and then accelerating over eastern China. Thus, the possibility that in
523 glacial times the jet remained south of Tibet seems plausible.

524 Because the annual cycles of precipitation and of $\delta^{18}\text{O}$ values differ from station
525 to station, we cannot argue that the differences in isotopes recorded in speleothems
526 among present-day, early Holocene, and glacial times will be the same throughout China.
527 In fact, it seems unlikely that a simple explanation of the kind offered above can account
528 for the full range of variations in speleothems. The simple arguments given in the
529 previous paragraph do suggest, however, that if different amplitudes of seasonal
530 variations cannot account for more than small fraction of the amplitude of variability seen
531 in speleothems, different durations of seasons may be an important factor that controls
532 variability on orbital time scales.

533

534 6. Conclusions

535 Modern station data offer little support for the idea that monthly or annual
536 variations in $\delta^{18}\text{O}$ values reflect variations in local precipitation on the same time scales,
537 and monthly data suggest that temperature variations correlate better with variations in
538 $\delta^{18}\text{O}$ values. Monthly $\delta^{18}\text{O}$ values correlate negatively with temperature – the same sign
539 of the correlation between $\delta^{18}\text{O}$ values in the cave records and the amplitude of insolation
540 ($\delta^{18}\text{O}$ values are more depleted during warmer times) – but are opposite to that expected
541 from the temperature dependence in Rayleigh fractionation. Monthly anomalies of $\delta^{18}\text{O}$
542 values, however, do not generally correlate well with monthly anomalies of temperature,

543 indicating that much of the covariance between $\delta^{18}\text{O}$ values and temperature is contained
544 in the seasonal cycle. Thus we infer that variation of $\delta^{18}\text{O}$ values and temperature on the
545 seasonal time scale primarily reflect independent processes each of which is regulated by
546 changes in insolation: local insolation directly regulates local temperature, and global
547 insolation gradients, correlated with local insolation, affect the source regions and
548 pathways of the $\delta^{18}\text{O}$ as it is delivered to the local site.

549 Cave speleothems, however, record a $\delta^{18}\text{O}$ signal of precipitation averaged over
550 several years. Modern station data averaged over 12 or 24 months do not show
551 significant variations between $\delta^{18}\text{O}_w$ values and temperature or precipitation at most
552 stations. Although one $\delta^{18}\text{O}$ record from 1953 to 2000 collected from Wanxiang cave
553 (Zhang et al., 2008) correlates negatively with local 5-year average precipitation and
554 positively with temperature, the magnitude of variation of $\delta^{18}\text{O}$ values on this timescale is
555 much smaller than that on orbital timescales.

556 If we assume that the $\delta^{18}\text{O}$ values from a paleoclimate record are a proxy for
557 precipitation amount, then we can make a crude estimate of the difference in precipitation
558 between present day and times in the past necessary to account for variability in $\delta^{18}\text{O}$
559 values in the paleoclimate record. Our calculations show that for a $\sim 1\%$ increase in $\delta^{18}\text{O}$
560 values, the difference between modern and 9 ka $\delta^{18}\text{O}$ values at Dongge and Hulu caves
561 (e.g., Wang et al., 2001; Yuan et al., 2004), annual precipitation 9 ka would be at least 1.5
562 times that of today. Calculations using atmospheric general circulation models estimate
563 this difference to be much smaller, around 10%. In light of the results above, we, like
564 others (e.g., Cai et al., 2006; Cheng et al., 2006; Dykoski et al., 2005; Johnson and
565 Ingram, 2004, Kelly et al., 2006; Wang et al., 2008; Yuan et al., 2004) conclude that

566 other processes – such as differences in re-evaporation, variations in atmospheric
567 circulation, and variations in rainstorm type – have as much influence on orbital scale
568 variability of $\delta^{18}\text{O}$ values in China as do precipitation amount or temperature. Similarly,
569 we argue that different, but plausible, amplitudes of the seasonal cycle of precipitation
570 amount and of $\delta^{18}\text{O}$ values can account for only a part, less than half, of the difference
571 between glacial and present-day $\delta^{18}\text{O}$ values.

572

573 The climatic cause of isotope fluctuations in Chinese speleothem records and the
574 nature of their link to the overall East Asian monsoon circulation remain open questions.
575 Several differences between past and present-day climates may combine to account for
576 the 3-6‰ amplitude of variability on orbital time scales. These include different values
577 in the oceans from which water is evaporated, different sources of moisture and different
578 pathways, different amounts of convective precipitation, which is highly depleted in ^{18}O ,
579 and different durations of seasons. Some of these processes may conspire together as
580 separate and even independent consequences of differences in large- and small-scale
581 atmospheric circulation, such as the seasonal cycle of the mid-latitude jet strength and
582 position and summer radiative heating over China, that result directly from differing
583 boundary conditions imposed by variations in isolation on a Milankovitch time scale and
584 from the effects of high-latitude ice sheets.

585

586 Appendix A. Simple scaling relationship

587 We perform a scale analysis to explore whether local precipitation differences,
588 arising either because of different amplitudes of annual precipitation or differing

589 amplitudes of the seasonal cycle, can plausibly explain the differences in $\delta^{18}\text{O}$ in the cave
590 records on orbital time scales. We assume that $\delta^{18}\text{O}$ values are a valid proxy for monthly
591 precipitation amounts and use empirical relationships between monthly precipitation and
592 monthly average $\delta^{18}\text{O}$ to ask: How much must annual precipitation amount or seasonality
593 change to produce the amplitude of $\delta^{18}\text{O}$ values in the paleorecords? The maximum
594 amplitude of the orbital timescale swings of $\delta^{18}\text{O}$ values from Dongge cave is $\sim 4 - 5\text{‰}$
595 near ~ 130 ka, the most recent minimum $\delta^{18}\text{O}$ value is $\sim -9\text{‰}$ at ~ 9 ka and the most
596 recent maximum $\delta^{18}\text{O}$ value is $\sim -5\text{‰}$ at ~ 15 ka, a difference of $\sim 4\text{‰}$ (Yuan et al., 2004).
597 For comparison the amplitude of variability in modern $\delta^{18}\text{O}$ values is $\sim 7 - 8\text{‰}$, and the
598 maximum peak-to-peak difference in $\delta^{18}\text{O}$ values in the modern speleothem record from
599 Wangxiang is only $\sim 0.3\text{‰}$ (Zhang et al., 2008).

600 We estimate annual $\delta^{18}\text{O}$ values for hypothetical past climates with mean annual
601 precipitation and seasonal amplitudes different from those day. We write monthly
602 precipitation as the sum of the annual average plus the monthly anomaly:

$$603 \quad P(t) = f_o P_o + f' P'(t) \quad (1)$$

604 where f_o and f' are factors that scale the annual mean and amplitude of seasonal
605 variability, respectively. For the modern day, $f_o = f' = 1$. For a climate where mean
606 annual precipitation is larger (smaller) than present, $f_o > 1$ ($f_o < 1$). For a climate with
607 wetter summers and drier winters (stronger monsoon) than present, $f' > 1$, and for a
608 climate with less seasonal variability (less monsoonal) than present, $f' < 1$.

609 We want to test the effects of different annual means f_o and the seasonal
610 amplitudes f' , assuming that $\delta^{18}\text{O}$ values scale with the monthly amount of precipitation.

611 We determine empirical relationships between monthly precipitation and monthly
612 average $\delta^{18}\text{O}$ values for each station using the station data. We fit $\delta^{18}\text{O}$ values as a
613 function of precipitation (Fig. 4) with straight lines, and use those lines to define the
614 relationship between $\delta^{18}\text{O}$ values and precipitation:

$$\begin{aligned} \delta_o &= aP_o + b \\ \delta'(t) &= aP'(t) \end{aligned} \quad (2)$$

616 where $a = \Delta\delta^{18}\text{O}/\Delta P$ is the slope of the best fit line and b is its y-intercept. Admittedly,
617 this method is crude – the modern data shows so much scatter that a linear fit may not be
618 reasonable (Fig. 4). The station-specific values of $a = \Delta\delta^{18}\text{O}/\Delta P$ calculated above,
619 however, are similar to those calculated by Bony et al. (2008) using a simple column-
620 integrated model for radiative-convective equilibrium over tropical ocean and by Lee et
621 al. (2008) using atmospheric GCM with an isotope model that includes a dependence of
622 isotopic content on precipitation amount during rainfall events (Lee et al., 2007).

623 We consider stations where monthly values of $\delta^{18}\text{O}$ and precipitation are
624 significantly correlated: Guiyang, Hong Kong, Kunming, and Zunyi, noting that others
625 also have used linear regressions to estimate changes in precipitation inferred from $\delta^{18}\text{O}$
626 records. For example, Johnson et al. (2006b) deduce that an 80% decrease in
627 precipitation is needed to explain a 3‰ reduction in $\delta^{18}\text{O}$ values in a record from
628 Wanxiang Cave, which is north of the northern limit of the Meiyu front, and they go on
629 to argue that dependences of $\delta^{18}\text{O}$ on the amount of precipitation or on local temperature
630 cannot account for the $\delta^{18}\text{O}$ record at this cave. Similarly, Kelly et al. (2006) require >
631 95% differences from present-day in precipitation to explain differences in glacial and
632 interglacial $\delta^{18}\text{O}$ values from Dongge cave.

633 If $P'(t)$ describes the seasonal cycle of precipitation, then the mean annual $\delta^{18}\text{O}$
 634 value, weighted by seasonal variations in precipitation, is:

$$635 \quad \delta_{ae}(t) = \frac{\int_0^{2\pi} P \delta dt}{\int_0^{2\pi} P dt}. \quad (3)$$

636 Suppose, first, that $P'(t)$ can be described with a cosine function,

$$637 \quad P'(t) = P_a \cos(t) \quad (4)$$

638 where P_a is the maximum monthly precipitation anomaly, then with substitution of (1),
 639 (2), and (4), (3) becomes:

$$640 \quad \delta_{ae} = af_o P_o + b + \frac{af'^2 P_a^2}{2f_o P_o} \quad (5)$$

641 The difference between a past climate state and the modern (for which δ_{ae} in (5) is given
 642 by substituting $f_o = f' = 1$) is:

$$643 \quad D = aP_o \left[(f_o - 1) + \frac{1}{2} \left(\frac{f'^2}{f_o} - 1 \right) \right]. \quad (6)$$

644 To simplify matters, we have assumed that $P_a = P_o$ in (6) (i.e., modern precipitation is P
 645 $= P_o(1 - \cos(t))$). We require that $|f'/f_o| \leq 1$ to ensure positive values of precipitation.

646 Note that the difference between past and modern climates is not dependent on b , defined
 647 in (2), because we have assumed that the relationship between $\delta^{18}\text{O}$ value and

648 precipitation is invariant with time. Using modern data to assign values to a and P_o for
 649 each station, we plot D as a function of mean annual precipitation amount f_o holding $f' =$

650 1 (Fig. 5a), D as a function of seasonal amplitudes of precipitation f' holding $f_o = 1$ (Fig.

651 5b), and D for the case where the mean annual and seasonal amplitude of precipitation

652 vary proportionally: $f = f' = f_o$ (Fig. 5c). The minimum f_o and maximum f' values that we

653 consider define limits beyond which the absolute value of the monthly precipitation
654 anomaly in the driest months of the year would be larger than the annual mean, resulting
655 in negative precipitation for the month. We also calculate D using the observed modern
656 seasonal cycles (Figure 1) instead of a cosine function in (4), and the resulting curves
657 differ only slightly in shape from those plotted in Fig. 5. Thus, insofar as modern scaling
658 of $\delta^{18}\text{O}$ on monthly precipitation amounts applies, variations in the shape of the seasonal
659 cycle have little effect on D .

660 The gray bands in Fig. 5a and 5c indicate minimum values of $\delta^{18}\text{O}$ values relative
661 to modern values from Hulu and Dongge caves (Yuan et al., 2004). To decrease the $\delta^{18}\text{O}$
662 value by 1‰ (the approximate difference between $\delta^{18}\text{O}$ values of present-day and 9 ka),
663 we estimate that the mean annual precipitation must be ~ 1.5 times larger than present at
664 Kunming and Zunyi, and as much as ~ 2 times larger than present at Hong Kong (Fig. 5a).
665 In the formulation presented above, changing the amplitude of the seasonal cycle cannot
666 cause a decrease of the $\delta^{18}\text{O}$ value by as much as 1‰, given the upper limit of f' (Fig.
667 5b). For the relative amount of summer to winter precipitation to increase sufficiently to
668 call for a 1‰ decrease in the $\delta^{18}\text{O}$ values, mean annual precipitation must be $>\sim 1.4$ times
669 larger than present at Kunming and Zunyi, and $>\sim 1.6$ times larger at Hong Kong (Fig.
670 5c).

671 We can also apply our analysis to the recent $\delta^{18}\text{O}$ record of Zhang et al. (2008)
672 from Wangxiang cave, assuming the seasonal cycle of precipitation there is reasonably
673 described by nearby stations Zunyi or Kunming. The maximum peak-to-peak difference
674 in their $\delta^{18}\text{O}$ record is a decrease of 0.3‰ between 1998 and 1986, when precipitation
675 increases from 320 mm/yr to 430 mm/yr (Zhang et al., 2008, Fig. S4). Using the simple

676 scaling law above and parameters appropriate for Zunyi or Kunming, a decrease of 0.3‰
677 implies a precipitation rate of 1.2 times 320 mm/yr, or ~380 mm/yr (Fig. 5a, 5c). In the
678 case of modern speleothem $\delta^{18}\text{O}$ records, therefore, the dependence on precipitation
679 amount underestimates the observed difference in precipitation. At the opposite extreme,
680 the small differences in $\delta^{18}\text{O}$ for relatively large variations of precipitation at Wangxiang
681 calls for absurdly large glacial-interglacial variations. The 110 mm/yr annual rainfall
682 difference correlated with a 0.3‰ in $\delta^{18}\text{O}$ values would require differences of >1000 mm
683 in annual rainfall at speleothem sites, when present-day annual precipitation is ~ 480 mm
684 (Zhang et al., 2008).

685

686 Appendix B. Comparison with General Circulation Model calculations

687 The failure of modern relationships between monthly $\delta^{18}\text{O}$ values and
688 precipitation amount pose the question of the relationship between $\delta^{18}\text{O}$ values and
689 climate variables on longer time scales differ from that for the present. GCMs can be
690 used to examine this from their calculated amounts of either precipitation or $\delta^{18}\text{O}$ values
691 vary in past climates. Several runs have been carried out with such tests in mind.

692 Using GCM experiments Kutzbach (1981) estimates ~ 10% greater summertime
693 precipitation and ~ 5% greater annually averaged precipitation amount at 9 ka than in
694 modern day. GCM ensemble results from the PMIP2 experiment show no significant
695 change in annual mean precipitation from 6 ka to present (Braconnot et al., 2007). By
696 comparison, our calculations above suggest that if a dependence on precipitation amount
697 is responsible for the difference in $\delta^{18}\text{O}$ values between the two times, the change in
698 precipitation amount must be much larger (Fig. 5a). Sustained differences of 50% or

699 more between present-day and modern annual precipitation seem unlikely, and thus these
700 calculations suggest that insofar as the modern dependence of $\delta^{18}\text{O}$ values on
701 precipitation applies to paleoclimate, summer precipitation amount cannot be the
702 explanation for the large variations in $\delta^{18}\text{O}$ values in speleothems in China.

703 We note also that most GCM runs that include stable isotopes of water predict
704 smaller differences between glacial and interglacial $\delta^{18}\text{O}$ values than those measured in
705 cave records. Calculated differences in $\delta^{18}\text{O}$ values in China from GCM simulations are
706 $\sim 2\text{‰}$ between the last glacial maximum and present (Hoffmann and Heiman, 1997,
707 Hoffmann et al., 2000, Jouzel et al., 1994), which are more than two small times smaller
708 than those observed in cave speleothems (Yuan et al., 2004). Recent simulations of $\delta^{18}\text{O}$
709 values over Holocene time by LeGrande and Schmidt (2009) do replicate approximately
710 the $\sim 1\text{‰}$ difference in this period, but they attribute this difference largely to differences
711 in vapor transport from the Pacific, not to precipitation amount or seasonal differences in
712 it.

713 Acknowledgments

714 We thank Larry Edwards, Scott Lehman, David Noone, and two anonymous
715 reviewers for thorough and constructive comments on previous versions of this
716 manuscript. Edwards, in particular, offered three unusually thorough reviews. This work
717 was funded by the US National Science Foundation, Continental Dynamics Program
718 (EAR-0507431). NCEP Reanalysis data provided by the NOAA/OAR/ESRL PSD,
719 Boulder, Colorado, USA from their website at <http://www.cdc.noaa.gov/>. Legates
720 Surface and Ship Observation of Precipitation data was obtained from the Goddard Earth
721 Sciences Data Information and Services Center: <http://daac.gsfc.nasa.gov/precipitation/>.
722 PMIP2 data was downloaded from their project website at <http://pmip2.lsce.ipsl.fr/>.

- 723 References
724
725 Abell, P. I., Hoelzmann, P., 2000. Holocene paleoclimates in northwestern Sudan: stable
726 isotope studies on mollusks. *Global and Planetary Change* 26, 1-12.
727
728 Arkin, H., Colton, R.R., 1970. *Statistical Methods*, Harper & Row, New York.
729
730 Bar-Matthews, M., Ayalon, A., Kaufman, A., 2000. Timing and hydrological conditions
731 of Sapropel events in the Eastern Mediterranean, as evident from speleothems,
732 Soreq Cave, Israel. *Chemical Geology* 169, 145-156.
733
734 Bar-Matthews, M., Ayalon, A., Gilmour, A., Matthews, A., Hawkesworth, C. J., 2003.
735 Sea-land oxygen isotopic relationships from planktonic foraminifera and
736 speleothems in the Eastern Mediterranean region and their implication for
737 paleorainfall during interglacial intervals. *Geochimica et Cosmochimica Acta* 67,
738 3181-3199.
739
740 Bony, S., Risi, C., Vimeux, F., 2008. Influence of convective processes on the isotopic
741 composition ($\delta^{18}\text{O}$ and δD) of precipitation and water vapor in the tropics: 1.
742 Radiative-convective equilibrium and the Tropical Ocean-Global Atmosphere-
743 Coupled Ocean-Atmosphere Response Experiment (TOGA-COARE) simulations.
744 *J. Geophys. Res.* 113, 10.1029/2008JD009942.
745
746 Braconnot, P., et al., 2007. Results of PMIP2 coupled simulations of the Mid-Holocene
747 and Last Glacial Maximum – Part 1: experiments and large-scale features.
748 *Climate of the Past* 3, 261-277.
749
750 Brown, D., Worden, J., Noone, D., 2008. Comparison of atmospheric hydrology over
751 convective continental regions using water vapor isotope measurements from
752 space. *J. Geophys. Res.* 113, doi:10.1029/2007JD009676.
753
754 Burns, S. J., Fleitmann, D., Matter, A., Kramers, J., Al-Subbary, A. A., 2003. Indian
755 Ocean climate and an absolute chronology over Dansgaard/Oeschger events 9 to
756 13. *Science* 301, 1365-1367.
757
758 Cai, Y., An, Z., Cheng, H., Edwards, R.L., Kelly, M.J., Liu, W., Wang, X., Shen, C.-C.,
759 2006. High-resolution absolute-dated Indian Monsoon record between 53 and 36
760 ka from Xiaobailong Cave, southwestern China. *Geology* 34, 621-624.
761
762 Cai, Y.-j., Tan, L.-c., Cheng, H., An, Z.-s., Edwards, R. L., Kelly, M. J., Kong, X.-g., and
763 Wang, X.-f., 2010. The variation of summer monsoon precipitation in central
764 China since the last deglaciation. *Earth and Planetary Science Letters* 291, 21-31.
765
766 Cheng, H., Edwards, R.L., Wang, Y.J., Kong, X.G., Ming, Y.F., Kelly, M.J., Wang, X.F.,
767 Gallup, C.D., Liu, W.G, 2006. A penultimate glacial monsoon record from Hulu
768 Cave and two-phase glacial terminations. *Geology* 34, 217-220.

769
770 Cheng, H., Edwards, R. L., Broecker, W. S., Denton, G. H., Kong, X-g., Wang, Y.-j.,
771 Zhang, R., Wang, X-f., 2009. Ice age terminations. *Science*, 236, 248-252.
772
773 Cobb, K. M., Adkins, J. F., Partin, J. W., and Clark, B., 2007. Regional-scale climate
774 influences on temporal variations of rainwater and cave dripwater oxygen
775 isotopes in northern Borneo. *Earth Planet. Sci. Lett.* 263, 207–220.
776
777 Cruz, F. W., Vuille, M., Burns, S. J., Wang, X.-f., Cheng, H., Werner, M., Edwards, R.
778 L., Karmann, I., Auler, A. S., Nguyen, H., 2009. Orbitally driven east–west
779 antiphasing of South American precipitation. *Nature Geosci.* 2, 210-214.
780
781 Dansgaard, W., 1964. Stable isotopes in precipitation. *Tellus* 16, 436-486.
782
783 Ding Yihui, Li Chongyin, Liu Yanju 2004. Overview of the South China Sea Monsoon
784 Experiment. *Advances in Atmospheric Sciences* 21, 343-360.
785
786 Dykoski, C.A., Edwards, R.L., Cheng, H., Yuan, D., Cai, Y., Zhang, M., Lin, Y., Qing,
787 J., An, Z., Revenaugh, J., 2005. A high-resolution, absolute-dated Holocene and
788 deglacial Asian monsoon record from Dongge Cave, China, *Earth Planet. Sci.*
789 *Lett.* 233, 71-86.
790
791 Emanuel, K., 2007. Quasi-Equilibrium Dynamics of the Tropical Atmosphere, in:
792 Schneider, T. Sobel, A. H. (Eds.), *The Global Circulation of the Atmosphere.*
793 Princeton University Press, Princeton, pp. 186-218.
794
795 Fairchild, I.J., Smith, C.L., Baker, A., Fuller, L., Spötl, C., Matthey, D., McDermott, F.,
796 E.I.M.F, 2006. Modification and preservation of environmental signals in
797 speleothems. *Earth Sci. Rev.* 75, 105-153.
798
799 Fasullo, J., Webster, P.J., 2003. A hydrological definition of Indian Monsoon onset and
800 withdrawal. *J. Climate* 16, 3200-3211.
801
802 Fleitmann, D., Burns, S. J., Mudelsee, M., Neff, U., Kramers, J., Mangini, A., Matter, A.,
803 2003. Holocene forcing of the Indian monsoon recorded in a stalagmite from
804 southern Oman. *Science* 300, 1737-1739.
805
806 Fleitmann, D., Burns, S. J., Neff, U., Mudelsee, M., Mangini, A., Matter, A., 2004.
807 Palaeoclimatic interpretation of high-resolution oxygen isotope profiles derived
808 from annually laminated speleothems from Southern Oman. *Quaternary Science*
809 *Reviews* 23, 935–945.
810
811 Gadgil, S., 2003. The Indian monsoon and its variability. *Annu. Rev. Planet. Sci.* 31, 429-
812 467.
813

814 Gat, J.R., 1996. Oxygen and hydrogen isotopes in the hydrologic cycle. *Annu. Rev. Earth*
815 *Planet. Sci.* 24, 225-262.
816

817 Guilderson, T. P., Fairbanks, R. G., Rubenstone, J. L., 2001. Tropical Atlantic coral
818 oxygen isotopes: glacial–interglacial sea surface temperatures and climate change.
819 *Marine Geology* 172, 75–89.
820

821 Hendy, C. H., 1971. The isotopic geochemistry of speleothems-I: The calculations of the
822 effects of different modes of formation on the isotopic composition of
823 speleothems and their applicability as paleoclimate indicators. *Geochimica et*
824 *Cosmochimica Acta* 35, 801–824.
825

826 Hoffmann, G., Heimann, M., 1997. Water isotope modeling in the Asian monsoon
827 region, *Quaternary International* 37, 115-128.
828

829 Hoffmann, G., Jouzel, J., Masson, V., 2000. Stable water isotopes in atmospheric general
830 circulation models. *Hydrological processes* 14, 1385-1406.
831

832 Holmgren, K., Lee-Thorp, J. A., Cooper, G. R. J., Lundblad, K., Partridge, T. C., Scott,
833 L., Sitaldeen, R., Talma, A. S., Tyson, P. D., 2003. Persistent millennial-scale
834 climatic variability over the past 25,000 years in Southern Africa. *Quaternary*
835 *Science Reviews* 22, 2311-2326.
836

837 Hu, C., Henderson, G.M., Huang, J., Xie, S., Sun, Y., Johnson, K.R., 2008.
838 Quantification of Holocene Asian monsoon rainfall from spatially separated cave
839 records. *Earth Planet. Sci. Lett.* 266, 221-232.
840

841 Huybers, P., 2006. Early Pleistocene glacial cycles and the integrated summer insolation
842 forcing. *Science* 313, 508-511.
843

844 IAEA/WMO, 2004. Global Network of Isotopes in Precipitation, The GNIP Database.
845 Accessible at: <http://isohis.iaea.org>
846

847 Johnson, K.R., Ingram, B.L., 2004. Spatial and temporal variability in the stable isotope
848 systematics of modern precipitation in China: implications for paleoclimate
849 reconstructions. *Earth Planet. Sci. Lett.* 220, 365-377.
850

851 Johnson, K.R., Hu, C., Belshaw, N.S., Henderson, G.M., 2006a. Seasonal trace-element
852 and stable-isotope variations in a Chinese speleothem: The potential for high-
853 resolution paleomonsoon reconstruction. *Earth Planet. Sci. Lett.* 244, 221-232.
854

855 Johnson, K.R., Ingram, B.L., Sharp, W.D., Zhang, P.Z., 2006b. East Asian summer
856 monsoon variability during Marine Isotope Stage 5 based on speleothem $\delta^{18}\text{O}$
857 records from Wanxiang Cave, central China. *Palaeogeogr. Palaeoclimatol.*
858 *Palaeoecol.* 236, 2-19.
859

860 Joussaume, S., Taylor, K.E., 1995. Status of the Paleoclimate Modeling Intercomparison
861 Project (PMIP), in Proceedings of the first international AMIP scientific
862 conference, WCRP Report, 425-430.
863

864 Jouzel, J., Koster, R.D., Suozzo, R.J., Russell, G.L., 1995. Stable water isotope behavior
865 during the last glacial maximum: A general circulation model analysis. *J.*
866 *Geophys. Res.* 99 25791-25801.
867

868 Kalnay, E., et al., 1996. The NCEP/NCAR 40-Year Reanalysis Project. *Bull. Am.*
869 *Meteorol. Soc.* 77, 437-472.
870

871 Kelly, M. J., Edwards, R.L., Cheng, H., Yuan, D., Cai, Y., Zhang, M., Lin, Y., An, Z.,
872 2006. High resolution characterization of the Asian Monsoon between 146,000
873 and 99,000 years B.P. from Dongge Cave and global correlation of events
874 surrounding Termination II. *Palaeogeogr. Palaeoclimatol. Palaeoecol.* 236, 20-38.
875

876 Kutzbach, J.E., 1981. Monsoon climate of the early Holocene: Climate experiment with
877 the earth's orbital parameters for 9000 years ago. *Science* 214, 59-61.
878

879 Lawrence, J. R., Gedzelman, S. D., 1996. Low stable isotope ratios of tropical cyclone
880 rains *Geophys. Res. Lett.* 23, 527-530.
881

882 Lawrence, J. R., Gedzelman, S. D., Dexheimer, D., Cho, H.-K., Carrie, G. D., Gasparini,
883 R., Anderson, C. R., Bowman, K. P., Biggerstaff, M. I., 2004. Stable isotopic
884 composition of water vapor in the tropics. *J. Geophys. Res.* 109, D06115,
885 doi:10.1029/2003JD004046.
886

887 Lee, E., Chase, T. N., Rajagopalan, B., 2008. Seasonal forecasting of East Asian summer
888 monsoon based on oceanic heat sources. *Int. J. Climatol.* 28, 667-678.
889

890 Lee, J.-E., Fung, I., DePaolo, D.J., Henning, C.C., 2007. Analysis of the global
891 distribution of water isotopes using the NCAR atmospheric general circulation
892 model. *J. Geophys. Res.* 112, doi:10.1029/2006JD007657.
893

894 Lee, J.-E., Fung, I., 2008. "Amount effect" of water isotopes and quantitative analysis of
895 post-condensation processes. *Hydrol. Process.* 22, 1-8.
896

897 Legates, D. R., Willmott, C. J., 1990. Mean seasonal and spatial variability in gauge-
898 corrected, global precipitation. *Int. J. Climatol.* 10, 111-127.
899

900 LeGrande, A. N., Schmidt, G. A., 2009. Sources of Holocene variability of oxygen
901 isotopes in paleoclimate archives. *Clim. Past* 5, 441-455.
902

903 Maher, B., 2008. Holocene variability of the East Asian summer monsoon from Chinese
904 cave records: a re-assessment. *The Holocene* 18, 861-866.
905

906 Molnar, P., Boos, W. R., Battisti, D. S., 2010. Orographic controls on climate and
907 paleoclimate of Asia: Thermal and mechanical roles for the Tibetan Plateau,
908 *Annu. Rev. Earth Planet. Sci.* 38, 77-102.
909

910 Oppo, D. W., Sun, Y. B., 2005. Amplitude and timing of sea-surface temperature change
911 in the northern South China sea: Dynamic link to the East Asian monsoon.
912 *Geology* 33, 785-788.
913

914 Risi, C., Bony, S., Vimeux, F., 2008. Influence of convective processes on the isotopic
915 composition ($\delta^{18}\text{O}$ and δD) of precipitation and water vapor in the tropics: 2.
916 Physical interpretation of the amount effect. *J. Geophys. Res.* 113,
917 doi:10.1029/2008JD009943.
918

919 Partin, J. W., Cobb, K. M., Adkins, J. F., Clark, B., Fernandez, D. P., 2007. Millennial-
920 scale trends in west Pacific warm pool hydrology since the Last Glacial
921 Maximum, *Nature*, 449, 452–455. doi:10.1038/nature06164.
922

923 Risi, C., Bony, S., Vimeux, F., Descroix, L., Ibrahim, B., Lebreton, E., Mamadou, I.,
924 Sultan, B., 2008. What controls the isotopic composition of the African monsoon
925 precipitation? Insights from event-based precipitation collected during the 2006
926 AMMA field campaign. *Geophys. Res. Lett.* 35, L24808,
927 doi:10.1029/2008GL035920.
928

929 Rozanski, K., Araguás-Araguás, L., Gonfiantini, R., 1992. Relation between long-term
930 trends of oxygen-18 isotope composition of precipitation and climate. *Science*
931 258, 981-985.
932

933 Schiemann, R., Lüthi, D., and Schär, C., 2009. Seasonal and interannual variability of the
934 westerly jet in the Tibetan Plateau region. *J. Climate* 22, 2940-2957. doi:
935 10.1175/2008JCLI2625.1.
936

937 Scholl, M. A., J. B. Shanley, J. P. Zegarra, and T. B. Coplen (2009), The stable isotope
938 amount effect: New insights from NEXRAD echo tops, Luquillo Mountains,
939 Puerto Rico, *Water Resour. Res.*, 45, W12407, doi:10.1029/2008WR007515.
940

941 Schrag, D. P., Adkins, J. F., McIntyre, K., Alexander, J. L., Hodell, D. A., Charles, C. D.,
942 McManus, J. F., 2002. The oxygen isotopic composition of seawater during the
943 Last Glacial Maximum. *Quaternary Science Reviews* 21, 331-342.
944

945 Severinghaus, J. P., 2009. Monsoons and meltdowns. *Science* 326, 240-241.
946

947 Sinha, A., Cannariato, K. G., Stott, L. D., Li, H.-C., You, C.-F., Cheng, H., Edwards, R.
948 L., Singh, I. B., 2005. Variability of Southwest Indian summer monsoon
949 precipitation during the Bølling-Ållerød. *Geology* 33, 813-816.
950

951 Sinha, A., Cannariato, K.G., Stott, L.D., Cheng, H., Edwards, R.L., Yadava, M.G.,
952 Ramesh, R., Singh, I.B., 2007. A 900-year (600 to 1500 A.D.) record of the
953 Indian summer monsoon precipitation from the core monsoon zone of India.
954 *Geophys. Res. Lett.* 34, doi:10.1029/2007GL030431.
955

956 Stute, M., Schlosser, P., Clark, J. F., Broecker, W.S., 1992. Paleotemperatures in the
957 southwestern United States derived from noble gas measurements in groundwater.
958 *Science* 256, 1000-1003.
959

960 Stute, M., Forster, M., Frischkorn, H., Serejo, A., Clark, J. F., Schlosser, P., Broecker, W.
961 S., Bonani, G., 1995. Cooling of tropical Brazil (5°C) during the last glacial
962 maximum. *Science* 269, 379-383.
963

964 Uppala, S. M., et al., 2005. The ERA-40 reanalysis, *Q. J. R. Meteorol. Soc.* 131, 2961–
965 3012.
966

967 Vaks, A., Bar-Matthews, M., Ayalon, A., Schilman, B., Gilmour, M., Hawkesworth, C.J.,
968 Frumkin, A., Kaufman, A., Matthews, A., 2003. Paleoclimate reconstruction
969 based on the timing of speleothem growth and oxygen and carbon isotope
970 composition in a cave located in the rain shadow in Israel. *Quaternary Research.*
971 59, 182-193.
972

973 Wang, B., Fan, Z., 1999. Choice of south Asian summer monsoon indices. *Bull. Amer.*
974 *Metero. Soc.* 80, 629-638.
975

976 Webster, P. J., Magaña, V.O., Palmer, T. N., Shukla, J., Tomas, R.A., Yanai, M.,
977 Yasunari, T., 1998. Monsoons: Processes, predictability, and the prospects for
978 prediction. *J. Geophys. Res.* 103, 14,451-14,510.
979

980 Wang, Y. J., Cheng, H., Edwards, R.L., An, Z.S., Wu, J.Y., Shen, C.-C., Dorale, J. A.,
981 2001. A high-resolution absolute-dated late Pleistocene monsoon record from
982 Hulu Cave, China. *Science* 294, 2345-2348.
983

984 Wang, Y.J., Cheng, H., Edwards, R.L., Kong, X.G., Shao, X.H., Chen, S.T., Wu, J.Y.,
985 Jiang, X.Y., Wang, X.F., An, Z.S., 2008. Millennial- and orbital-scale changes in
986 the East Asian monsoon over the past 224,000 years. *Nature* 451, 1090-1093.
987

988 Yamada, H., Geng, B., Uyeda, H., Tsuboki, K., 2007. Role of the heated landmass on the
989 evolution and duration of a heavy rain episode over a Meiyu-Baiu frontal zone. *J.*
990 *Metero. Soc. Japan* 85, 687-709.
991

992 Yuan, D.X., Cheng, H., Edwards, R.L., Dykoski, C.A., Kelly, M.J., Zhang, M.L., Qing,
993 J.M., Lin, Y.S., Wang, Y.J., Wu, J.Y., Dorale, J.A., An, Z.S., Cai, Y.J., 2004.
994 Timing, duration and transition of the last interglacial Asian Monsoon. *Science*
995 304, 575-578.
996

- 997 Zhang, P., Cheng, H., Edwards, R.L., Chen, F., Wang, Y., Yang, X., Liu, J., Tan, M.,
998 Wang, X., Liu, J., An, C., Dai, Z., Zhou, J., Zhang, D., Jia, J., Jin, L., Johnson,
999 K.R., 2008. A test of climate, sun, and culture relationships from an 1810-year
1000 Chinese cave record. *Science* 322, 940-942.
1001
- 1002 Zhou, W.-j., Priller, A., Beck, J. W., Wu Zhengkun, Chen Maobai, An Zhisheng, W.
1003 Kutschera, Xian Feng, Yu Huagui, Liu Lin, 2007. Disentangling geomagnetic and
1004 precipitation signals in an 80-kyr Chinese loess record of ^{10}Be . *Radiocarbon* 49,
1005 139–160.
1006
- 1007 Zhou, Y., Gao, S., Shen, S.S.P., 2004. A diagnostic study of formation and structures of
1008 the Meiyu Front System over East Asia. *J. Meteor. Soc. Japan* 82, 1565-1576.
1009

1010 Table caption

1011

1012 Table 1: Correlation coefficients r and partial correlation coefficients ρ calculated for
1013 $\delta^{18}\text{O}$ values and precipitation P and temperature T from nine GNIP stations. Sample size
1014 is n . Coefficients that are significant at the 95% confidence interval are printed in bold
1015 italics. A reduced degrees of freedom of $(n/3)-2$ is used in the monthly correlations to
1016 account for autocorrelation in the records, which is significant for one or two month lags.

1017

1018

1019 Figure captions

1020

1021 Figure 1: Elevation map of China and surrounding areas with locations of GNIP stations
1022 used in this study. Dongge, Hulu, Heshang, and Xiaobailong cave locations are marked
1023 with black dots. Insets show seasonal cycles of temperature (red lines, units of $^{\circ}\text{C}$, left
1024 axis), precipitation (blue lines, units of cm/month , left axis), and $\delta^{18}\text{O}$ values (black lines,
1025 units of ‰ , right axis). Dashed line indicates approximate northern limit of Meiyu front
1026 (Zhou et al., 2004).

1027

1028 Figure 2: Annual mean (1920-1980) precipitation rate (mm/day) over southeast Asia
1029 from the Legates Surface and Ship Observation of Precipitation dataset (Legates and
1030 Willmott, 1990). Black contour lines denote elevations of 0 m and 2000 m. Note high
1031 precipitation rates along the Himalayan front and in southeast China resulting from South
1032 Asian and East Asian monsoon activity.

1033

1034 Figure 3: Spatial correlation of annual mean precipitation (left) and temperature (right)
1035 between a given site (top: Hulu cave, middle: Dongge cave, bottom: East India) and the
1036 rest of Asia. Correlation coefficient is shown in filled contours, and correlations
1037 significant at a 95% confidence interval are outlined by the black contour. Precipitation
1038 and temperature from NCAR/NCEP Reanalysis (Kalnay et al. 1996).

1039

1040 Figure 4: Monthly total precipitation (mm , squares) and monthly mean temperature ($^{\circ}\text{C}$,
1041 diamonds) versus monthly mean $\delta^{18}\text{O}$ values (‰) for stations at (a) Fuzhou, (b) Guilin,
1042 (c) Guiyang, (d) Hong Kong, (e) Kunming, (f) Liuzhou, (g) Nanjing, (h) Shijiazhuang,
1043 and (i) Zunyi, whose locations are shown in Figure 1. Linear regressions used in the
1044 calculations in the Discussion are shown in black lines for stations at Guiyang, Hong
1045 Kong, Kunming, and Zunyi.

1046

1047 Figure 5: Calculated annual average weighted $\delta^{18}\text{O}$ values relative to modern, D , as a
1048 function of (a) f_o for $f' = 1$, (b) f' for $f_o = 1$, and (c) $f = f_o = f'$ calculated using equation (6)
1049 relative to modern values. Dotted lines (marked 'G') are calculations for station at
1050 Guiyang, dashed lines (marked 'HK') are for Hong Kong, dot-dashed lines (marked 'K')
1051 are for Kunming, and solid lines (marked 'Z') are for Zunyi. Grey bands in (a) and (c)
1052 indicate minimum $\delta^{18}\text{O}$ values in the records from Dongge and Hulu caves (2004).
1053 Values for a and P_o in equation (2) for the stations shown are: $a = -0.025$, $P_o = 80.4$
1054 (Guiyang); $a = -0.0081$, $P_o = 196.1$ (Hong Kong); $a = -0.03$, $P_o = 83.0$ (Kunming); and a

1055 = -0.030, $P_o = 81.5$ (Zunyi). Units of a and P_o are %/mm/month and mm/month,
1056 respectively.
1057

Figure

[Click here to download Figure: figures_012110.pdf](#)

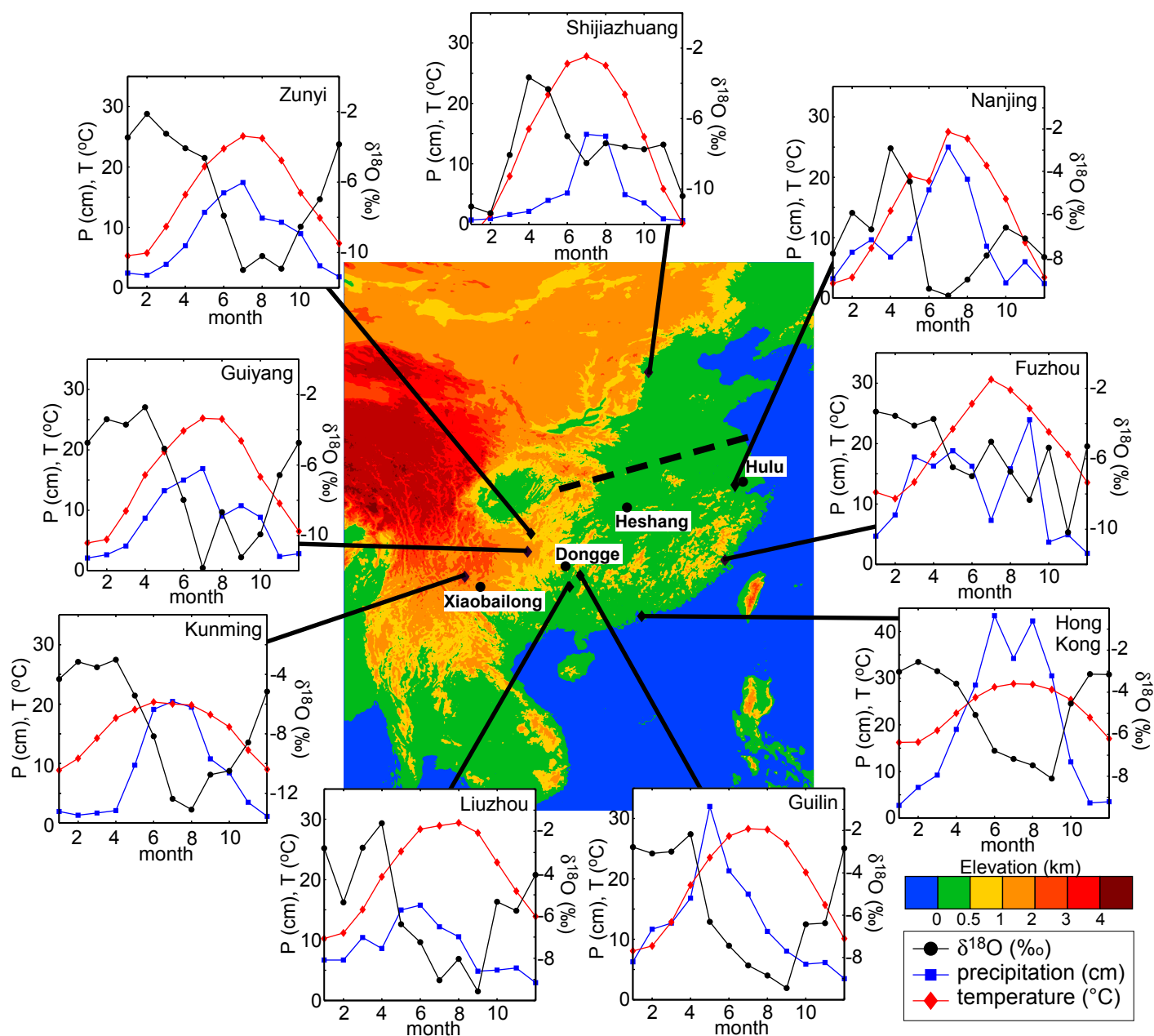


Figure 1: Elevation map of China and surrounding areas with locations of GNIP stations used in this study. Dongge, Hulu, Heshang, and Xiaobailong cave locations are marked with black dots. Insets show seasonal cycle of temperature T (red lines, units of $^{\circ}\text{C}$, left axis), precipitation P (blue lines, units of cm/month , left axis), and $\delta^{18}\text{O}$ values (black lines, units of ‰, right axis). Dashed line indicates approximate northern limit of Meiyu front (Zhou *et al.*, 2004).

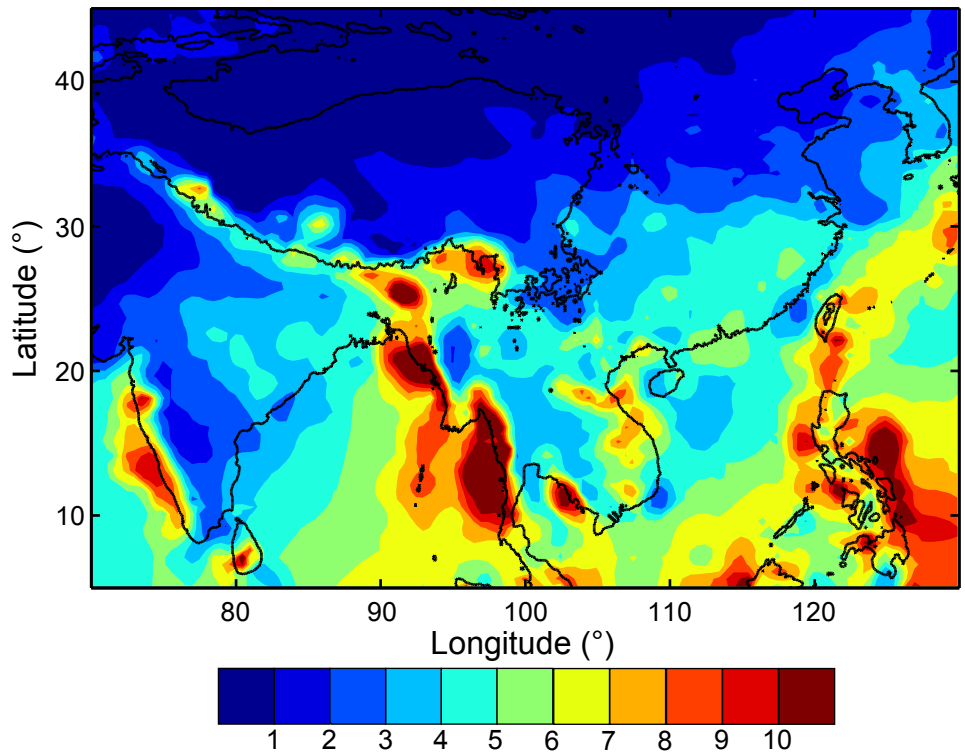


Figure 2: Annual mean (1920-1980) precipitation rate (mm/day) over southeast Asia from the Legates Surface and Ship Observation of Precipitation dataset (Legates and Willmott, 1990). Black contour lines denote elevations of 0 m and 2000 m. Note high precipitation rates along the Himalayan front and in southeast China resulting from Indian and East Asian monsoon activity.

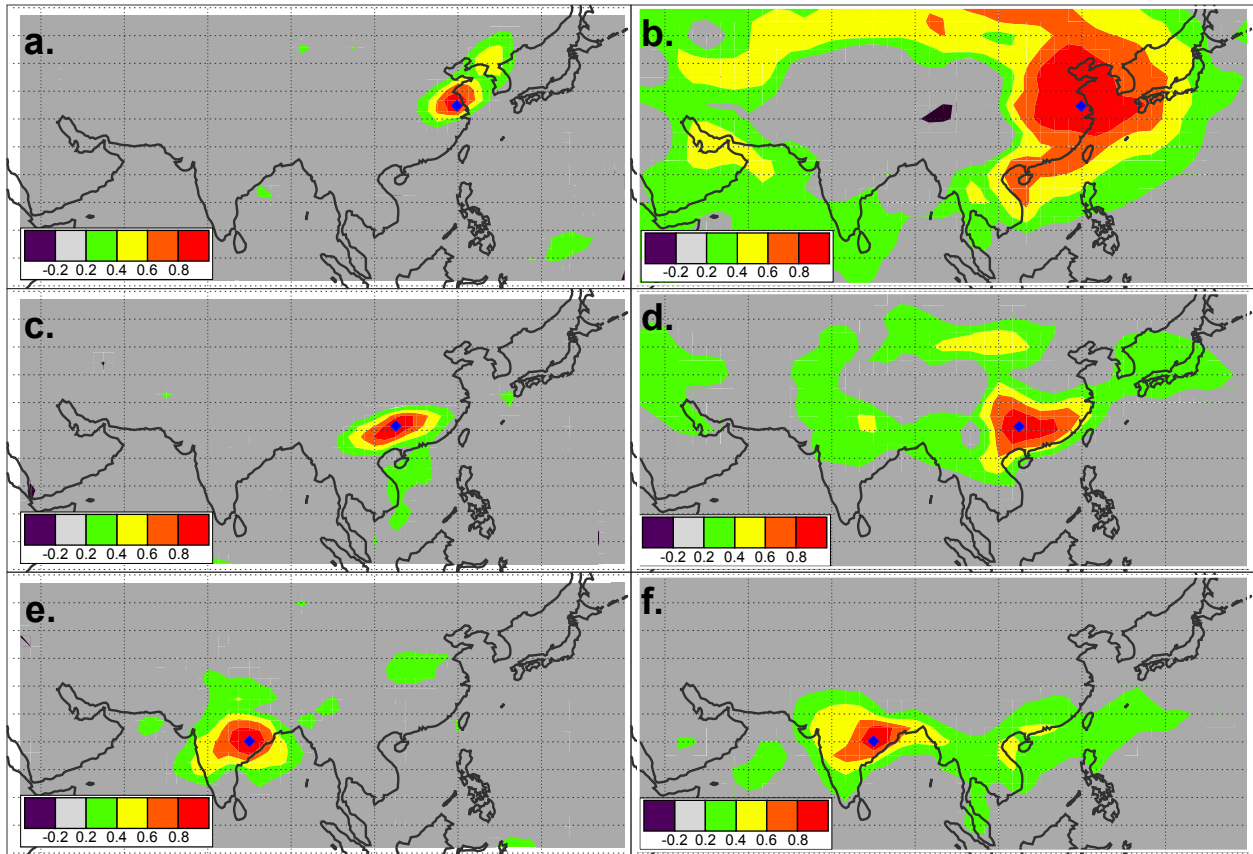


Figure 3: Spatial correlation of yearly average precipitation (left) and temperature (right) between a given site (top: Hulu cave, middle: Dongge cave, bottom: East India) and the rest of Asia. Correlation coefficient is shown in filled contours, and correlations significant at a 95% confidence interval are colored. Grey areas indicate insignificant correlations. Precipitation and temperature from NCAR/NCEP Reanalysis (Kalnay et al., 1996).

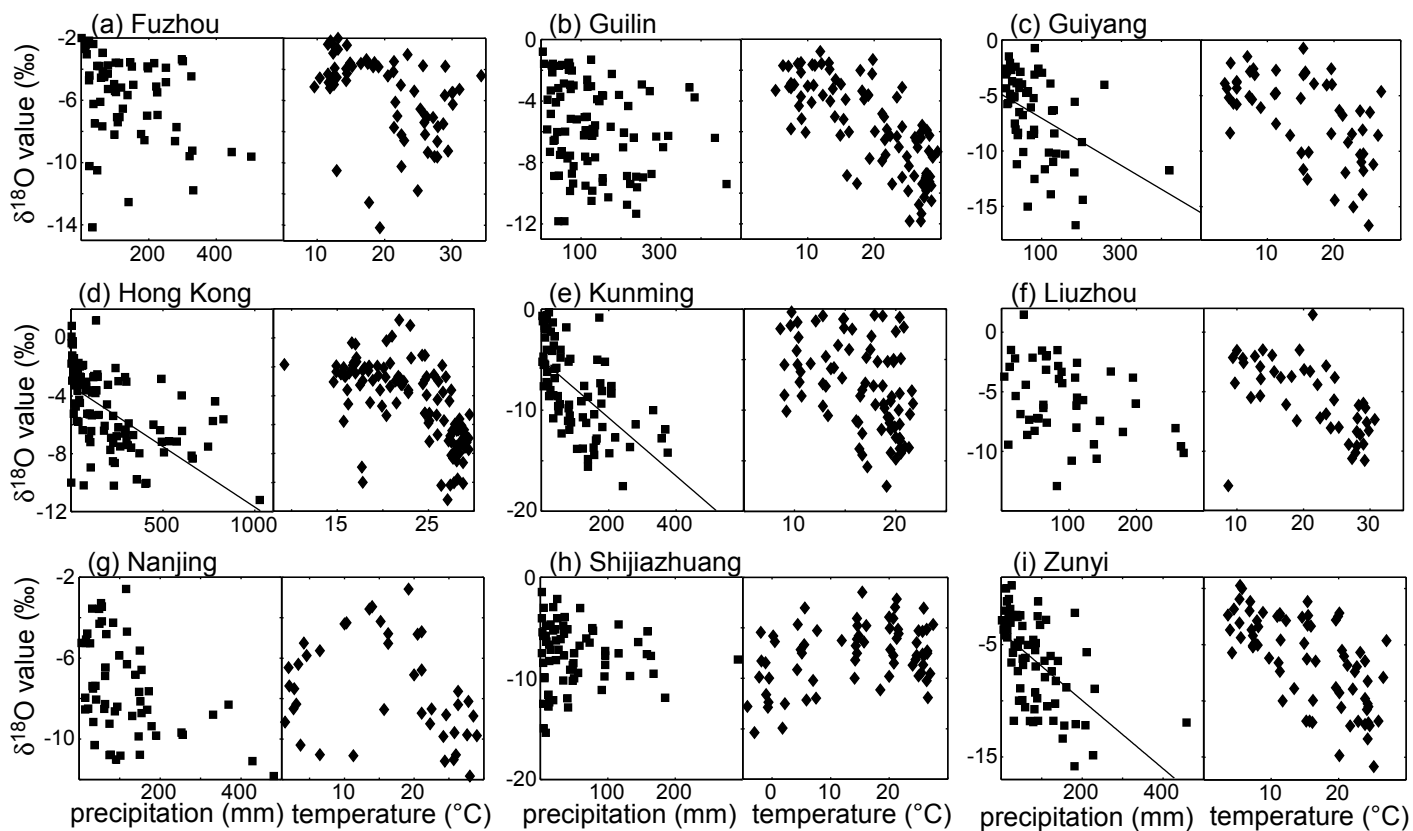


Figure 4: Monthly total precipitation (mm, squares) and monthly mean temperature (°C, diamonds) versus monthly mean $\delta^{18}\text{O}$ values (‰) for stations at (a) Fuzhou, (b) Guilin, (c) Guiyang, (d) Hong Kong, (e) Kunming, (f) Liuzhou, (g) Nanjing, (h) Shijiazhuang, and (i) Zunyi. Linear regressions used in the calculations in the Discussion are shown in black lines for stations at Guiyang, Hong Kong, Kunming, and Zunyi.

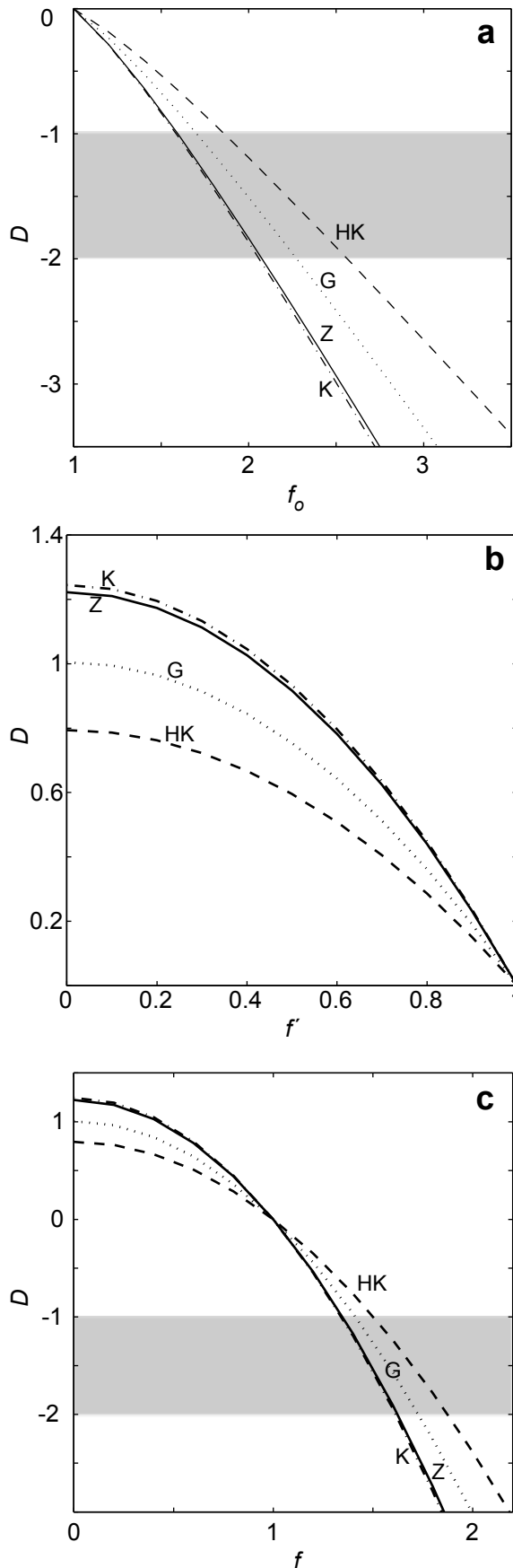


Figure 5: Annual average weighted $\delta^{18}\text{O}$ value relative to modern, D , as a function of (a) f_0 for $f' = 1$, (b) f' for $f_0 = 1$, and (c) $f = f_0 = f'$ calculated using equation (6) relative to modern values. Dotted line (marked 'G') is calculation for station at Guiyang, dashed line (marked 'HK') is Hong Kong, dot-dashed line (marked 'K') is Kunming, and solid line (marked 'Z') is Zunyi. Grey bands in (a) and (c) indicate minimum $\delta^{18}\text{O}$ values in the records from Dongge and Hulu caves (2004). Values for a and P_0 in equation (2) for the stations shown are: $a = -0.025$, $P_0 = 80.4$ (Guiyang); $a = -0.0081$, $P_0 = 196.1$ (Hong Kong); $a = -0.03$, $P_0 = 83.0$ (Kunming); and $a = -0.030$, $P_0 = 81.5$ (Zunyi). Units of a and P_0 are $\text{‰}/\text{mm}/\text{month}$ and mm/month , respectively.

Table

[Click here to download Table: dayem_table1_090909.pdf](#)

station	monthly average		monthly anomaly		monthly average partial correlations		n
	$r(\delta^{18}\text{O},\text{P})$	$r(\delta^{18}\text{O},\text{T})$	$r(\delta^{18}\text{O},\text{P})$	$r(\delta^{18}\text{O},\text{T})$	$\rho(\delta^{18}\text{O},\text{P},\text{T})$	$\rho(\delta^{18}\text{O},\text{T},\text{P})$	
Fuzhou	-0.35	-0.38	-0.36	-0.08	-0.29	-0.33	71
Guilin	-0.20	-0.72	-0.18	0.00	0.09	-0.71	92
Guiyang	-0.48	-0.57	-0.31	0.11	-0.22	-0.40	58
Hong Kong	-0.61	-0.67	-0.33	-0.03	-0.36	-0.47	276
Kunming	-0.61	-0.44	-0.09	0.23	-0.48	-0.11	152
Liuzhou	-0.37	-0.55	-0.42	0.37	-0.27	-0.50	45
Nanjing	-0.45	-0.25	0.06	-0.07	-0.39	0.02	58
Shijiazhuang	-0.09	0.38	-0.20	0.30	-0.35	0.49	146
Zunyi	-0.56	-0.65	-0.34	0.07	-0.25	-0.44	70